Aqueous seeded RAFT polymerization for the preparation of self-assemblies containing nucleobase analogues

Miriam Abad, [a,b] Martina Nardi, [c] Luis Oriol, [a,b] Milagros Piñol *[a,b] and Eva Blasco *[d,e]

[a.] Instituto de Nanociencia y Materiales de Aragón (INMA), CSIC-Universidad de Zaragoza, Zaragoza 50009, Spain. E-mail: mpinol@unizar.es

[b.] Departamento de Química Orgánica, Facultad de Ciencias, Universidad de Zaragoza, Pedro Cerbuna, 12, Zaragoza 50009, Spain

[c.] Institute of Nanotechnology (INT), Karlsruhe Institute of Technology (KIT), Hermann-von-Helmholtz-Platz 1, Eggenstein-Leopoldshafen 76344, Germany

[d.] Organic Chemistry Institute, University of Heidelberg, In Neuenheimer Feld 270, 69120, Germany. E-mail: eva.blasco@oci.uni-heidelberg.de

[e.] Institute for Molecular Systems Engineering and Advanced Materials, University of Heidelberg, In Neuenheimer Feld 225, 69120 Germany

Self-assemblies containing the nucleobase analogue 2,6-diacylaminopyridine (DAP) have been successfully prepared for the first time by aqueous seeded RAFT polymerization in high concentrations. For this purpose, a diblock copolymer containing poly(ethylene glycol) (PEG) and DAP polymethacrylate blocks was used as a macro chain transfer agent (**PEG$_{124}$-b-PDAP$_9$-CTA**) for the polymerization of 2-hydroxypropyl methacrylate (HPMA) in water. From the systematic variation of the degree of polymerization and solids concentration, a phase diagram has been generated that correlates both variables with the morphologies of this new system. Self-assemblies have been characterized by TEM and DLS, observing morphologies from low to high order (from spherical micelles to worms and to vesicles). Self-assemblies morphologies are stable for almost a year, except in the case of worms that turn into spherical micelles after a few weeks. In addition, H-bonding supramolecular functionalization of the DAP repeating units during aqueous seeded RAFT polymerization has been examined by functionalization with a cross-linker with four thymine groups. Finally, the loading and the subsequent release of Nile Red has been proven in both supramolecular cross-linked and non-cross-linked self-assemblies.

Introduction

Amphiphilic block copolymers (BCs) are able to self-assemble in aqueous media leading to different structures with size at the nanoscale and potential uses in diverse fields including the biomedical one.[1,2] The morphology and size of amphiphilic BCs self-assemblies is frequently tailored by adjusting the length of each block, their chemical structure and the processing methodology.[1] The majority of these self-assembly methodologies, such as thin-film rehydration,[3] solvent displacement,[4,5] sonication[6] or microfluidics,[7] are post-polymerization processes that in some cases consist of time-consuming multiple steps and usually provide highly diluted BC dispersions (below 1 wt.%). Over the past years, polymerization-induced self-assembly (PISA) has emerged as an attractive one-step alternative where self-assembly occurs during the polymerization, thus avoiding multiple processing or purification steps and also providing highly concentrated self-assemblies dispersions (up to 50 wt.%) with good colloidal stability. Besides, adjusting the polymerization conditions, PISA allows access to self-assemblies with morphologies from low to high order (e.g. from spherical micelles to worms and to vesicles).[8–10]

Among the controlled radical polymerizations suitable for PISA, reversible addition-fragmentation chain-transfer (RAFT) polymerization has been the most widely exploited thanks to metal-free condition, its high tolerance to functional groups and the possibility to obtain well-defined architectures with, predetermined molar masses, low dispersities and end-group fidelity.[9,11] Commonly, a macro chain transfer agent (macro-CTA) is employed for the PISA

polymerization to grown a BC that self-assembles *in situ*. Depending on the solubility of both the macro-CTA and the monomer, emulsion RAFT polymerization,[12] dispersion RAFT polymerization[13–18] or seeded RAFT polymerization[19] are possible. The latter and more recent uses an amphiphilic BC macro-CTA that self-assembles at the polymerization medium acting as a seed or nanoreactor for a third block chain extension. Depending on the solubility of the monomer employed, and the resultant polymeric chain, seeded RAFT polymerization can be categorized in different types.[19–22]

Even though PISA self-assemblies are usually stable in the polymerization medium, the conditions of the environment in which they perform their function (i.e. presence of non-selective solvents, proteins, surfactants or very dilute media) can compromise their stability. Therefore, covalent cross-linking[18] either during polymerization, employing divinyl monomers,[23–28] or by either chemical[29–32] or photochemical[33,34] activated post-polymerization processes has been reported to enhance the nanoparticles stability. However, supramolecular or non-covalent cross-linking has been a less explored alternative despite being an easy and more versatile approach. In addition, its dynamic nature can be advantageous for certain applications like drug delivery. Examples of PISA incorporating non-covalent interactions have been described with either electrostatic,[35] host-guest[36,37] or hydrogen bonding interactions. In particular, hydrogen bonding interactions have been studied not only as cross-linking interactions[38,39] but also as driver for template interaction,[14,16,40,41] and even responsible of upper critical solution temperature (UCST) behavior.[42]

Among suitable monomers for aqueous dispersion RAFT polymerization, 2-hydroxypropyl methacrylate (HPMA) has been widely studied since it is a water-miscible monomer (up to 13 w/v % at room temperature) that forms a water-insoluble polymer.[15] PISA polymerization of HMPA has been approached using several macro-CTAs or hydrophilic stabilizer blocks such as poly(glycerol methacrylate),[15,23,27–29,43,44] poly(2-(methacryloyloxy)ethyl phosphorylcholine)[26] or poly(ethylene glycol) (PEG)[13,17,30,33,43,45–48] or even statistical copolymers like poly(glycerol methacrylate-*st*-glycidyl methacrylate).[31,36]

For some time now, our group has worked on the synthesis and self-assembly of linear-linear[7,49,50] and linear-dendritic[51] amphiphilic BCs containing a PEG hydrophilic block and a hydrophobic one bearing the 2,6-diacylaminopyridine (DAP) unit, which is a nucleobase analogue able to form multiple hydrogen bonds, for different purposes. Furthermore, PEG has been recurrently employed in biomedical application given that it is non-toxic and able to reduce immunogenicity, which enables the extension of *in vivo* circulation lifetimes for any encapsulated molecules.[52] These DAP-containing amphiphilic BCs exhibited excellent self-assembly behavior forming homogeneous dispersions of micelles or vesicles either by solvent-switching or microfluidics. And their potential as nanocarriers has been evaluated using fluorescent probes,[7,49–51] or camptothecin[49] and naproxen[7] as drug models. The cell viability of these systems was confirmed on several cell lines as well as the pH[49] and light-stimulated[50] release of the cargoes, in the last case using thymine-containing azocompounds as photoresponsive moieties supramolecularly linked to DAP units. Recently, this outstanding self-assembly behavior has been exploited to process hybrid systems consisting of plasmonic Pd(0) nanosheets, grown inside of polymeric micelles, for photothermal therapy under NIR stimulation.[7]

In order to further exploit the potential of incorporating nucleobases analogues such as DAP units into amphiphilic BCs, this work explores the preparation of highly concentrated aqueous self-assemblies dispersions using the PISA methodology as well as the supramolecular H-

bonding functionalization of the formed self-assemblies. Although there are some examples on the dispersion RAFT polymerization of nucleobases, such as the polymerization of adenine- and thymine-containing monomers in chloroform or dioxane by Kang *et. al*,[14,16] to the best of our knowledge neither nucleobase nor nucleobase analogues have been employed in RAFT-PISA in water. One of the reasons is the often poor water solubility of the nucleobase-containing monomers. Thus, a new strategy has been designed herein to integrate DAP units into a BC which is then employed as macro-CTA for the aqueous seeded RAFT polymerization of HPMA. Moreover, the feasibility of supramolecular functionalization has been demonstrated using a cross-linker with thymine terminal moieties to induce self-assembly and supramolecular cross-linking in one-pot.

Results and discussion

Synthesis of DAP-containing macro-CTA and self-assembly behavior

The direct incorporation of the DAP-containing methacrylic monomer in an aqueous RAFT polymerization system was not obvious, since it is poor soluble in water but also in several tested water/miscible organic solvent mixtures (see SI). To face this challenge, a different approach was adopted where PEG-CTA is chain extended with DAP to form a BC macro-CTA subsequently employed for aqueous RAFT polymerization of HPMA (Scheme 1). Indeed, HPMA is commercialized as a mixture of 2-hydroxypropyl methacrylate and 1-hydroxypropan-2-yl methacrylate so, strictly speaking, the resulting polymeric block is a statistical copolymer of the two isomers.
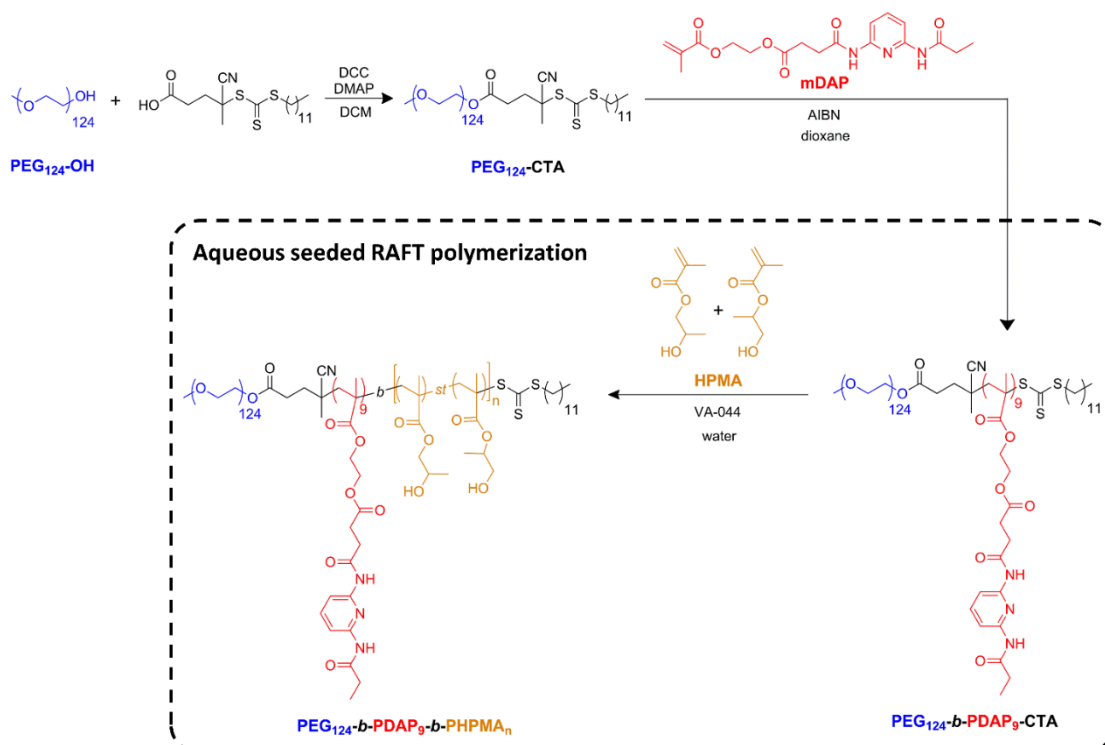

Scheme 1. Synthesis of **PEG$_{124}$-*b*-PDAP$_9$-CTA** macro-CTA by RAFT polymerization, and **PEG$_{124}$-*b*-PDAP$_9$-*b*-PHPMA$_n$** by aqueous seeded RAFT polymerization.

In this way, a diblock copolymer macro-CTA with a PEG and a PDAP blocks was first synthesized in two steps (Scheme 1) by RAFT polymerization. Commercial PEG monomethyl ether (**PEG$_{124}$-**

OH, 5450 g mol^{-1}) was first conjugated with 4-cyano-4-[(dodecylsulfanylthiocarbonyl)sulfanyl]pentanoic acid by a Steglich esterification reaction to obtain the corresponding **PEG$_{124}$-CTA**. This chain-transfer agent was chosen since it is suitable for (meth)acrylates polymerization.[53,54] **PEG$_{124}$-CTA** was characterized by GPC (Fig. S1) and the successful incorporation of the CTA was verified by ^{1}H NMR spectroscopy (Fig. S2). In a second step, the BC **PEG$_{124}$-b-PDAP$_9$-CTA** was prepared by RAFT polymerization (Scheme 1) of the methacrylic monomer **mDAP** from **PEG$_{124}$-CTA**.[55] Based on our experience, the target degree of polymerization of the PDAP block was limited to 10 to ensure an adequate water compatibility of the resulting BC macro-CTA. Experimental degree of polymerization and average molar mass (M_n) of the resulting diblock copolymer were determined by ^{1}H NMR spectroscopy (Fig. S3) being 9 and 9440 g mol^{-1} respectively. The polymer was also characterized by GPC and a low polydispersity was found ($Đ$ = 1.18) (Fig. S1).

The resulting BC, **PEG$_{124}$-b-PDAP$_9$-CTA,** was directly dispersed in water forming transparent solutions up to 10 g of polymer per 100 mL of water. Due to its amphiphilic character, the possible self-assembly in water was evaluated by transmission electron microscopy (TEM) (Fig. 1) and dynamic light scattering (DLS) (Fig. S4). Short worms coexisting with a small population of spherical micelles of 15 ± 4 nm diameter were observed by TEM at 0.1 g per 100 mL polymer concentration (Fig. 1a). The self-assembly behavior of **PEG$_{124}$-b-PDAP$_9$-CTA** in mixtures of water and HPMA was also studied simulating the aqueous RAFT polymerization conditions (T = 50°C). Two mixtures containing [HPMA]/[**PEG$_{124}$-b-PDAP$_9$-CTA**] = 100 and 300 molar ratios at a solids content of 10 g in 100 mL of water were evaluated that correspond to molar ratios and concentration feed in the aqueous RAFT polymerization (see below). The TEM images indicated that worms were shortened, and spherical micelles of 15 ± 4 nm diameters were predominant in the first mixture (Fig. 1b). However, by increasing the concentration of HPMA, it was found that the worms disappeared and spherical micelles were larger in size (27 ± 10 nm) and dispersity (Fig. 1c). DLS measurements of the self-assemblies were also performed at the polymerization temperature (50°C) and it was observed that the presence of HPMA decreased the apparent D_h (Fig. S4). Therefore, when the macro-CTA and HPMA were dispersed together in water, the initial **PEG$_{124}$-b-PDAP$_9$-CTA** preferentially formed spherical micelles.
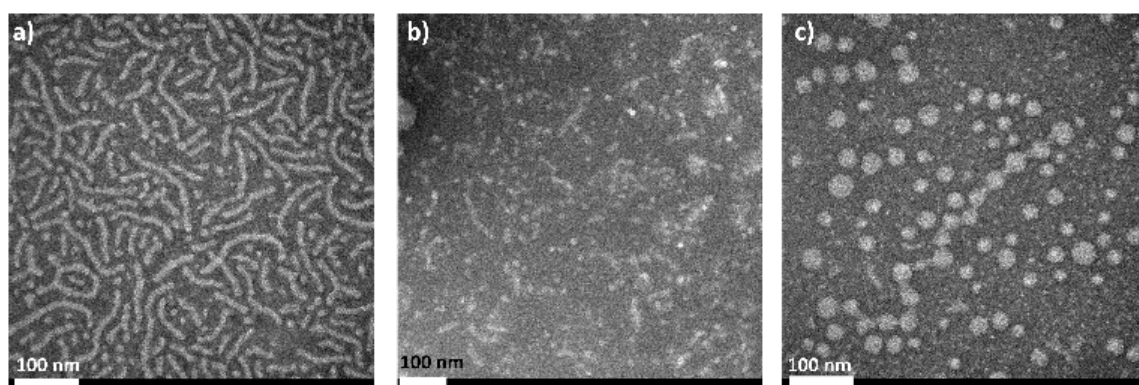
Fig. 1. (a) TEM images of self-assemblies formed in water by **PEG$_{124}$-b-PDAP$_9$-CTA** at 0.1 g per 100 mL. TEM images of self-assemblies formed in water for (b) [HPMA]/[**PEG$_{124}$-b-PDAP$_9$-CTA**] = 100 ratio and (c) [HPMA]/[**PEG$_{124}$-b-PDAP$_9$-CTA**] = 300 ratio at a content of 10 g of solids in 100 mL of water.

Aqueous seeded RAFT polymerization and morphological characterization of self-assemblies

Since it is expected that the CTA group is embedded inside the micelles core (hydrophobic part) after self-assembly, chain extension to form the third HMPA block (PHMPA) should occur mainly inside the micelles. To check this HMPA migration, ^{1}H NMR spectra were recorded for HPMA and a mixture of HPMA and **PEG$_{124}$-*b*-PDAP$_9$-CTA**, both in D$_2$O (Fig. S5). An attenuation in the signals was observed for the mixture of HPMA and **PEG$_{124}$-*b*-PDAP$_9$-CTA** compared to signals of HPMA. This fact suggested a HPMA migration into **PEG$_{124}$-*b*-PDAP$_9$-CTA** self-assemblies as reported in literature for other systems.[56] Therefore, the self-assemblies would act as seeds for the polymerization of the water soluble HPMA monomer. Thus, polymerization of HMPA using the macro-CTA **PEG$_{124}$-*b*-PDAP$_9$-CTA** can be properly considered as a seeded dispersion RAFT polymerization in water.[19]

The aqueous seeded RAFT polymerization of HMPA using **PEG$_{124}$-*b*-PDAP$_9$-CTA** (Scheme 1) was initiated by 2,2'-azobis[2-(2-imidazolin-2-yl)propane] dihydrochloride (VA-044) at 50°C. A 0.3 molar ratio between initiator and macro-CTA ([VA-044]/[**PEG$_{124}$-*b*-PDAP$_9$-CTA**]) was employed. This ratio was previously reported as optimum for aqueous RAFT-PISA of HMPA using **PEG$_{124}$-CTA** to obtain well defined copolymers with relatively low dispersity and minimal homopolymer contamination.[13] Polymerization was maintained for 5 h.

The influence of the polymer concentration and the length of the hydrophobic segments on the self-assembling properties were investigated performing three series of experiments, x = 1, 2 and 3, where the target degree of polymerization given by [HPMA]/[**PEG$_{124}$-*b*-PDAP$_9$-CTA**] ratio was approx. n = 100, 200 and 300, respectively. For each series, polymerization was performed at different solids concentrations (c = 10, 15, 20 and 25 expressed as grams of solids per 100 mL of water).). 25 g/100 mL was determined to be the maximum concentration at which **PEG$_{124}$-*b*-PDAP$_9$-CTA** was well dispersed in water before precipitating. Experiments were coded as c-x, where c refers to the solids concentration and x refers to the series of polymers. In all cases very high HPMA conversion values (≥ 98%) were obtained (Table S1), as calculated by ^{1}H NMR (Fig. S6), using DMF as internal standard.[17]

Polymers were analyzed by GPC (Fig. 2 and S7, and Table S1). GPC traces of the prepared polymers showed similar average molar masses for BCs with PHPMA of comparable length prepared at different polymer concentrations (Fig. 2). Dispersity values were in all cases between 1.31-1.45, higher than that of **PEG$_{124}$-*b*-PDAP$_9$-CTA** (Đ = 1.18). Nonetheless, it was observed that combining high target PHPMA degrees of polymerization and low solids concentrations favored the apparition of a small shoulder at higher elution times. GPC measurements were carried out at different polymer concentrations to dismiss the presence of self-assemblies in the eluent. Thus, shoulders should be most likely attributed to the presence of residual **PEG$_{124}$-*b*-PDAP$_9$-CTA**[44,46] due to a relative low degree of uncontrolled polymerization at higher PHPMA degrees of polymerization and lower solids concentration.

The morphology of the self-assemblies prepared by aqueous seeded RAFT polymerization was identified by TEM and cryo-TEM while average hydrodynamic diameters (D_h) and polydispersity indexes (PDI) were determined by DLS (Table 1). The resulting phase diagram is shown in Fig. 3.

For series x = 1, having an approx. target polymerization degree of n = 100, turbid but fluid homogeneous dispersions of micelles were obtained for all tested polymerization concentrations (i.e. from c = 10 to 25 g solids/100 mL of water) with average D_h values around

40 nm that were larger than those of **PEG$_{124}$-*b*-PDAP$_9$-CTA**, and low PDI (< 0.1). Taking these observations as a starting point, transitions to more ordered morphologies from spherical micelles-to-worms-to-vesicles were detected with increasing both the length of the PHPMA block, i.e., the hydrophobic content of the final BCs, and the total solids concentration.
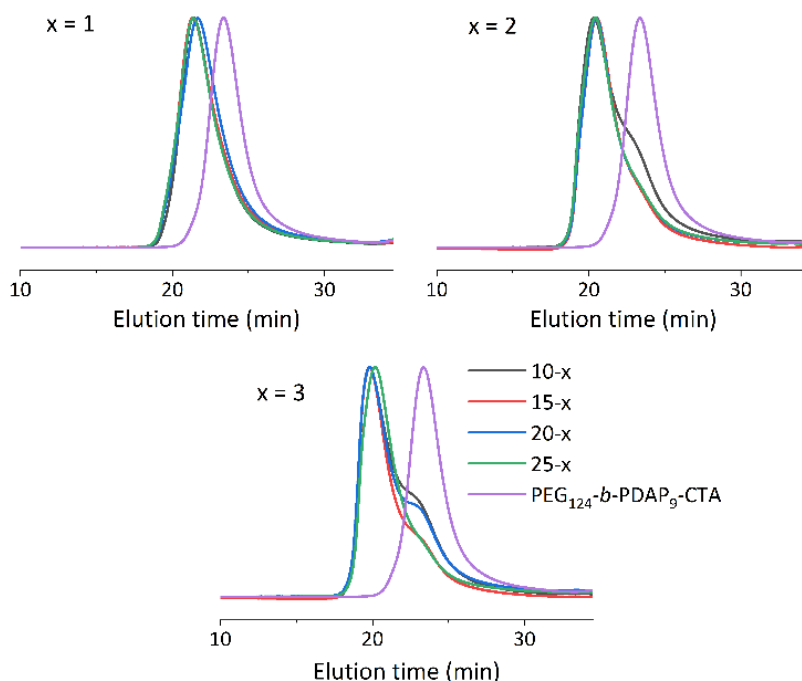

Fig. 2. GPC chromatograms of series x = 1-3, polymerized at c = 10, 15, 20 and 25 solids concentrations. Eluent: DMF (LiBr 50 mM). Detector: UV (290 nm).

For instance, when fixing the solids concentration at c = 10 g/100 mL but increasing the target degree of polymerization, an increase of the turbidity of the collected dispersions was observed with the naked eye. Accordingly, for **10-2** spherical homogeneous micelles of a larger size were self-assembled, with average D_h increasing from 39 ± 9 nm for **10-1** to 70 ± 20 nm for **10-2** (Fig. S8). Then, unilamellar vesicles were identified by Cryo-TEM for **10-3** (Fig. 4) with sizes ranging from 55 to 350 nm (average D_h = 164 ± 57 nm) and membrane thickness of 21 ± 2 nm. For **10-3**, remaining spherical micelles were also observed by TEM.

Considering higher solids concentrations (c = 15, 20 and 25 g/100 mL) and high target degree of polymerization (series x = 2 and 3), opaque white viscous dispersions with intermediate or even more complex and mixed self-assemblies morphologies were produced. For **15-2**, **20-2** and **25-2**, worms of approx. 35 nm cross section were predominately detected in TEM images with some residual spherical micelles. The high viscosity of dispersions with a soft gel like appearance, can probably be associated to a network formation due to entanglements of the worms.[57] By DLS (Fig. S8), broad size distributions with large PDI values were registered. Nonetheless, DLS analysis should be taken with care for worm-like particles since D_h are estimated under the assumption that particles exist in solution as compact spheres.

For samples of series x = 3, more complex morphologies were observed by TEM (Fig. 3) and Cryo-TEM (Fig. 4) above a concentration 10 g/100 mL, consisting of mixture of unilamellar and oligolamellar vesicles, or vesicles within vesicles, with sizes going from a few hundred nm to a few μm and 25-30 nm membranes thickness. Vesicles with sizes above 1 μm appeared as broken or folded even in Cryo-TEM. The folding of such large vesicles even in Cryo-TEM is not unusual since the vitrified ice layer should only be around a few 100 nm. In addition, some worms and

intermediate morphologies of worm-to-vesicle transitions such as wormballs and jellyfish-like geometries were observed (Fig. S9).[15]
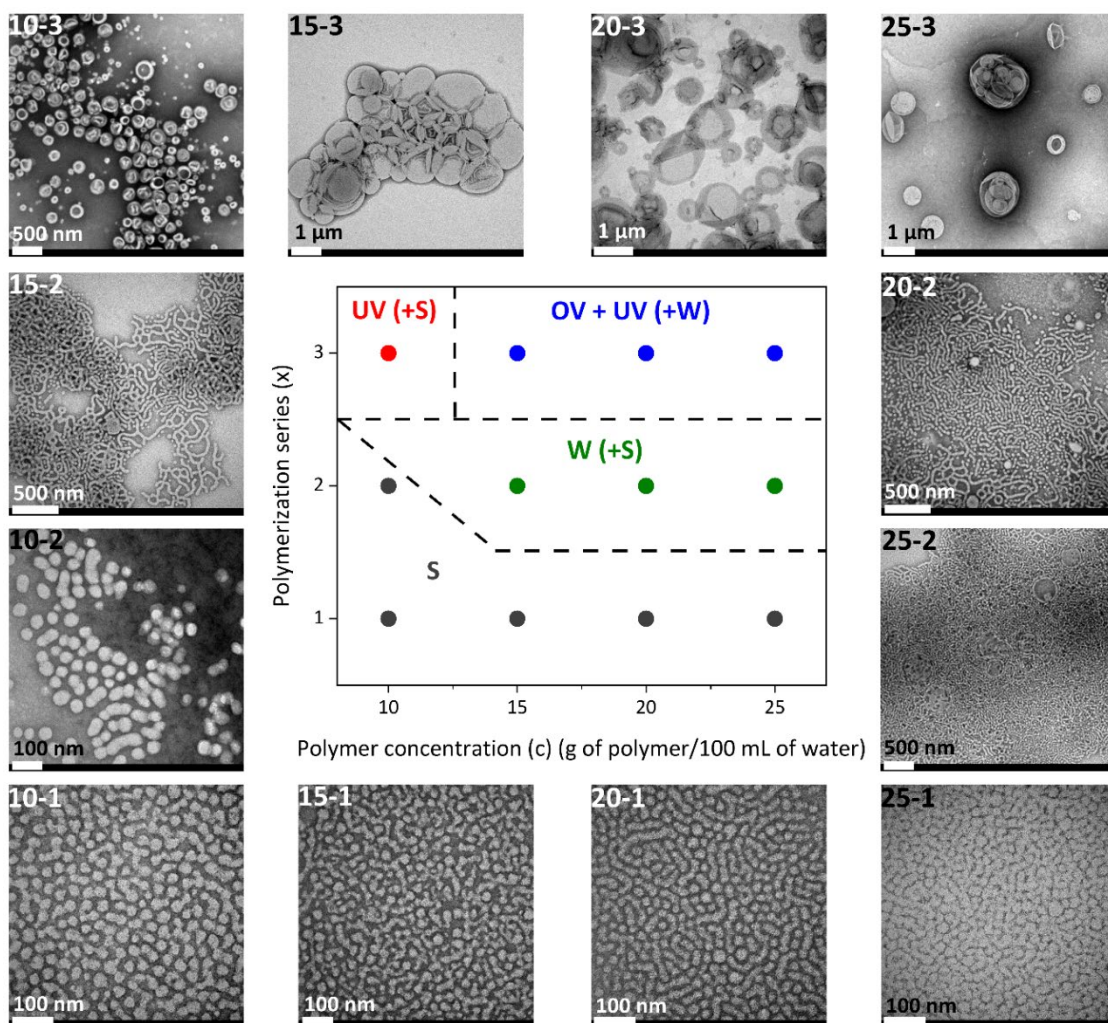
Fig. 3. Phase diagram of **PEG$_{124}$-*b*-PDAP$_9$-*b*-PHPMA$_n$** self-assemblies dispersions prepared, accompanying TEM images (S = spheres or spherical micelles; W = worms; UV = unilamellar vesicles; OV = oligolamellar vesicles).

Despite the presence of PDAP block, the results obtained in the morphological characterization data of **PEG$_{124}$-*b*-PDAP$_9$-*b*-PHPMA$_n$** self-assemblies dispersions prepared by aqueous seeded RAFT polymerization were in accordance with the ones from BCs prepared by aqueous dispersion RAFT polymerization, using PEG as macro-CTA and HPMA as monomer.[13,17]

The stability of the dispersions upon storage was evaluated by DLS up to 11 months (Fig. S10). Those dispersions with self-assembled spherical micelles (**10-1**, **15-1**, **20-1**, **25-1** and **10-2**) and unilamellar vesicles (**10-3**) were stable as concluded from registered DLS curves, with only a slightly increase in average D_h and PDI for samples **10-1** and **15-1** due to some aggregation of the micelles as observed by TEM (Figure S11) after 11 months. For those samples containing oligolamellar vesicles or vesicles within vesicles (**15-3**, **20-3** and **25-3**) only slight variations were observed along the time. However, a clear evolution was observed after 6 weeks for dispersions containing worms (**15-2**, **20-2** and **25-2)** with a remarkable decrease of the apparent D_h. However, DLS measurements taken at the 12th week were similar to those of the 6th week. (Fig. S12a). After 12 weeks, TEM images showed a large population of spherical micelles coexisting with short worms (Fig. S12b). This suggests the worm dissociation into cylindrical and spherical

micelles, which might be more thermodynamically stable morphologies.[13,43] Not a significant further evolution of the samples was observed after 11 months.

Table 1. Characterization data obtained for **PEG$_{124}$-b-PDAP$_9$-b-PHPMA$_n$** self-assemblies dispersions.

Sample	M$_n$[a] (kDa)	Hydrophilic/ hydrophobic ratio[b]	D$_h$ (PDI)[c] (nm)	TEM size[d] (nm)	Morphology
10-1	26.0	21/79	39±9 (0.02)	25±6	Spherical micelles
10-2	40.3	13/87	70±20 (0.07)	44±9	Spherical micelles
10-3	58.2	9/91	164±57 (0.10)	55-350[e]	Unilamellar vesicles
15-1	24.6	22/78	40±11 (0.06)	29±7	Spherical micelles
15-2	41.0	13/87	326±178 (0.29)	33±6	Worms (+ spheres)
15-3	57.9	9/91	883±422 (0.19)	220-1750[e]	Oligolamellar vesicles
20-1	25.5	21/79	38±12 (0.10)	21±6	Spherical micelles
20-2	40.7	13/87	436±169 (0.37)	32±9	Worms (+ spheres)
20-3	56.5	10/90	949±489 (0.24)	100-1500[e]	Oligolamellar vesicles
25-1	24.5	22/78	41±11 (0.05)	25±6	Spherical micelles
25-2	40.2	14/86	883±551 (0.47)	37±8	Worms (+ spheres)
25-3	54.7	10/90	906±540 (0.34)	95-1500[e]	Oligolamellar vesicles

[a] Average number molar mass (M$_n$) calculated considering for **PEG$_{124}$-b-PDAP$_9$-CTA** M$_n$ = 9440 g mol^{-1} (estimated by ^{1}H NMR) and the PHPMA degree of polymerization. [b] Hydrophobic/hydrophilic weight percentage ratio estimated considering the PEG block as the hydrophilic part and the **PDAP$_9$-b-PHPMA$_n$** segment as the hydrophobic part. [c] Average D$_h$ values and PDI provided by Zetasizer software, from the intensity particle size distribution recorded by DLS. [d] TEM size data was reported as the mean ± SD (standard deviation) of 150 measurements histogram. [e] Mean size and SD could not be reported since the histogram obtained did not fit to a Gaussian curve.
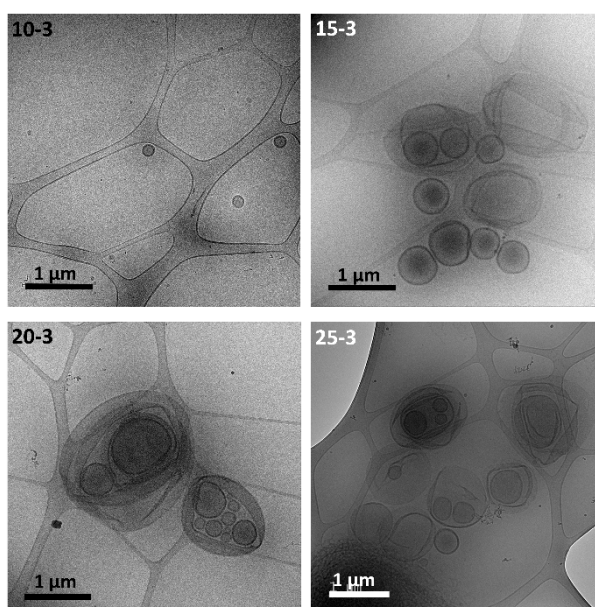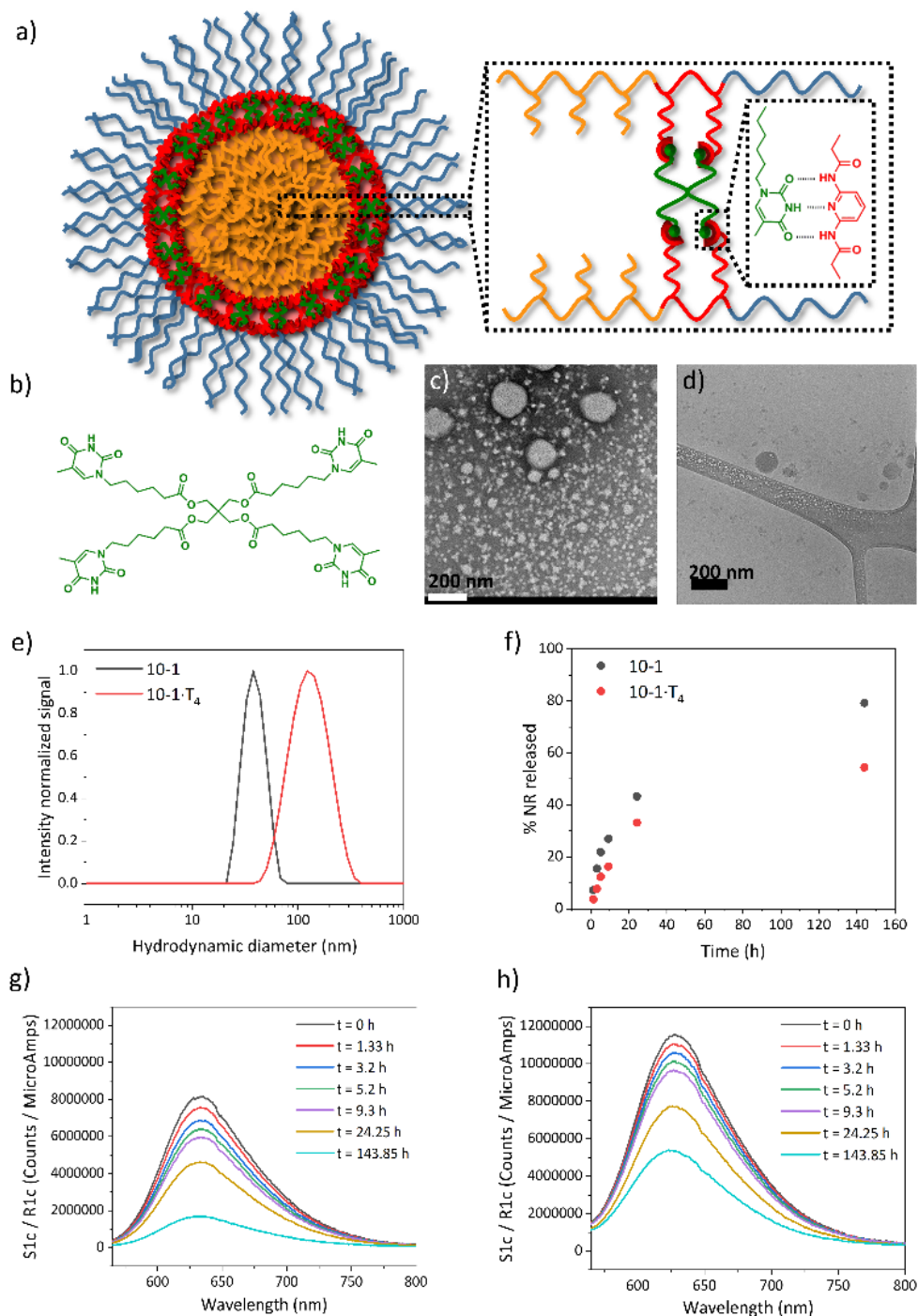

Fig. 4. Cryo-TEM images from **PEG$_{124}$-b-PDAP$_9$-b-PHPMA$_n$** dispersions of series x = 3, obtained at different solids concentrations (c = 10, 15, 20 and 25).

Functionalization of the DAP-containing self-assemblies with a thymine cross-linker

As a next step, the ability of DAP-containing self-assemblies to be functionalized by supramolecular recognition of thymine derivatives mediated by a triple H-bonding was exploited (Fig. 5a). In particular, a molecule containing four thymine units (T_4) (Fig. 5b) was employed as a cross-linker to improve the stability of the self-assemblies in water. It is expected that the incorporation of T_4 plays a key role in potential application of these system as nanocarriers.

Fig. 5. (a) Supramolecular recognition through a triple H-bond between DAP units (red) from **PEG$_{124}$-b-PDAP$_9$-b-PHPMA$_n$** and thymine moieties (green) of the cross-linker (**T$_4$**). (b) Chemical structure of cross-linker (**T$_4$**). (c) TEM and (d) Cryo-TEM images of **10-1·T$_4$** self-assemblies. (e) Intensity particle size distributions recorded by DLS of **10-1** and **10-1·T$_4$** self-assemblies dispersions. (f) Release kinetics curves of NR encapsulated into **10-1** and **10-1·T$_4$**. Fluorescence spectra of NR loaded (g) **10-1** and (h) **10-1·T$_4$** self-assemblies at different dialysis times.

In order to incorporate the thymine derivative **T₄** into the system, one-pot seeded polymerization and supramolecular cross-linking were carried out. In particular, we performed an analogous experiment to **10-1** sample targeting a degree of polymerization of approx. 100 (series x = 1) and a final polymer concentration c = 10 (resulting material coded **10-1·T₄**) using a **T₄:PEG₁₂₄-*b*-PDAP₉-CTA** molar ratio of 2.2:1 (*i.e.* a 1:1 thymine:DAP ratio). Because **T₄** is not soluble in water, it was incorporated into the small amount of DMF employed as internal standard in the polymerization process (see details in the experimental section). Previous to seeded aqueous polymerization, the influence of **T₄** on the initial self-assemblies of **PEG₁₂₄-*b*-PDAP₉-CTA** and, **PEG₁₂₄-*b*-PDAP₉-CTA** and **HPMA** mixture was tested by TEM (Figure S13) observing that **T₄** induced the transformation to shorter worms and more spherical micelles in the first case while only spherical micelles were observed if HPMA was present. Polymerization was conducted to a high conversion (98%; Table S1) similar to **10-1** sample.

This time the envisaged self-assembly and supramolecular cross-linking resulted in a milky appearance dispersion for **10-1·T₄** in contrast to the translucent dispersion collected for **10-1**. GPC analysis (Fig. S14) gave a low dispersity value, Đ = 1.31, in analogy to **10-1**. Notwithstanding, GPC curves show two polymer distributions, one of them at the same elution time as the corresponding non-cross-linked sample, and another at higher elution time. This suggests that the HPMA polymerization is hindered to some extent by the presence of **T₄**. By TEM (Fig. 5c), spherical micelles with a diameter of 21 ± 3 nm, smaller in size than the corresponding non-cross-linked ones, were observed, and they tend to aggregate. These micelles coexist with big spheres having sizes between 125-200 nm that seemed to have a compact and solid core as it was suggested by Cryo-TEM (Fig. 5d). These big spheres contribution in DLS shifted mean size distribution to higher D_h value (D_h= 137 ± 55 nm) (Fig. 5e). Therefore, the presence of **T₄** during the polymerization seemed to affect the polymerization and consequently the morphology of the self-assemblies formed.

Having stablished the conditions for the preparation of supramolecular cross-linked self-assemblies in water, the influence of cross-linking on the encapsulation and release of small molecular cargoes was investigated. Nile Red (NR) was selected as a hydrophobic molecular fluorescent probe. First, NR was encapsulated by diffusion in **10-1** and **10-1·T₄** samples. NR loaded dispersions were characterized by DLS and TEM (Fig. S15). By DLS only one size distribution was observed in both cases, very similar to the corresponding plain samples. Also by TEM, similar morphologies were observed with only a slight increase in the average size for **10-1+NR**, from 25 to 29 nm when compared to **10-1**. As it was seen by fluorescence spectroscopy (Fig. 5g-h), a higher amount of NR was encapsulated into **10-1·T₄** than into **10-1**, around 1.4 times more. To evaluate the NR release, both dispersions were dialyzed against a large water volume following NR fluorescence evolution as it is related to the NR still encapsulated. As it can be seen in Fig. 5f, NR release was slower for **10-1·T₄** than for **10-1**, which evidences the higher stability of supramolecular cross-linked self-assemblies comparing to non-cross-linked ones.

Experimental

Materials

Poly(ethylene glycol) monomethyl ether (**PEG₁₂₄-OH**) with a molar mass of 5000 g mol⁻¹ was purchased from Polysciences (Polysciences Europe GmbH, Hirschberg an der Bergstrasse, Germany) and its commercially reported average molar mass and polydispersity were checked by ^{1}H NMR (degree of polymerization = 124; M_n = 5450 g mol⁻¹; Fig. S16) and by mass

spectrometry (M_n determined by Polytools Bruker software for the analysis of mass spectrometry data = 5320 g mol^{-1}). 4-Cyano-4-[(dodecylsulfanylthiocarbonyl)sulfanyl]pentanoic acid (97%) (CTA) was purchased from Merck (Merck KGaA, Darmstadt, Germany) and used as received. Methacrylate monomer **mDAP** was synthesized following previously reported procedures.[55] 2,2'-Azobis(2-methylpropionitrile) (AIBN) was purchased from Merck and recrystallized in ethanol before use. Dioxane was purchased from Merck and passed through a basic alumina column prior to use. 2,2'-Azobis[2-(2-imidazolin-2-yl)propane] dihydrochloride (VA-044) was purchased from TCI (TCI Europe N.V., Zwijndrecht, Belgium). The monomer 2-hydroxypropyl methacrylate (97%, mixture of isomers 2-hydroxypropyl methacrylate and 1-hydroxypropan-2-yl methacrylate, **HPMA**) was purchased from Merck and passed through a basic alumina column to remove inhibitor prior to use. Four thymine-terminal groups supramolecular cross-linker (**T₄**) was synthesized following previously report procedures.[51] Chloroform-d₃ (CDCl$_3$, 99.8 atom % D), methanol-d₄ (MeOD, 99.8 atom % D) and water-d₂ (D$_2$O, 99.9%D) were purchased from Merck and utilized as solvent for NMR measurements. Other reagents were purchased from Merck and used as received.

Characterization techniques and instrumentation

^{1}H NMR, either in CDCl$_3$, MeOD or D$_2$O, were performed using a Bruker Avance III 300 spectrometer (Bruker, Billerica, MA, USA) operating at 300 MHz proton frequency, or in a Bruker Avance III 400 Prodigy spectrometer operating at 400 MHz proton frequency, at 25°C using standard pulse sequences. Chemical shifts are given in ppm relative to TMS, and the solvent residual peak was used as an internal reference. MALDI-TOF mass spectrometry was performed on a Microflex Bruker mass spectrometer, employing dithranol as matrix. Gel permeation chromatography (GPC) was performed using a Water Alliance 2695 liquid chromatography system equipped with a UV-vis-Waters 2998 Photodiode Array detector and two columns Styragel (HR1, 100Å and HR3, 1000Å) from Waters (5 μm, 7.8x300 mm) using DMF HPLC grade, with LiBr 50 mM, as eluent (0.5 mL min^{-1}) applying a calibration with polystyrene standards. Samples were prepared taking an aliquot of the polymer dispersion that was first lyophilized and then dissolved into the eluent (DMF (LiBr 50 mM)).

Dynamic Light Scattering (DLS) measurements were carried out in a Malvern Instrument Nano Zs (Malvern, Worcestershire, UK) using a He-Ne laser with a 633 nm wavelength and a detector angle of 173° at 25°C. The aqueous self-assemblies dispersions were measured at approximately 1.0 mg mL^{-1} concentration, and hydrodynamic diameters (D_h) were given as an average of three measurements on each sample to ensure reproducibility. Transmission Electron Microscopy (TEM) analysis were developed in a FEI Tecnai T20 microscope (FEI Company, Waltham, MA, USA) operating at 200 kV. TEM samples were prepared adding 10 μL of each self-assemblies' dispersion at approximately 1.0 mg mL^{-1} concentration on a continuous carbon film-copper grid, and the excess was removed by capillarity using filter paper. Then, the grids were stained with uranyl acetate (1% aqueous solution), removing the excess again by capillarity using filter paper. The grids were dried overnight under vacuum. Cryogenic Transmission Electron Microscopy (Cryo-TEM) analysis were developed in a JEM-2011 microscope (Jeol Europe SAS, Croissy-sur-Seine, France) operating at 80 kV. For Cryo-TEM, holey carbon film-copper grids previously ionized using a plasma cleaner were employed. A droplet was placed onto the grid, and sample vitrification was automatically processed using FEI Vitrobot and carried out in liquid ethane. Samples were kept under liquid nitrogen with a Gatan TEM cryo-holder (FEI Company). Fluorescence emission spectra were performed using a Fluorolog FL3-11 spectrometer (HORIBA ABX SAS, Madrid, Spain), using a Front Face accessory.

Macro-CTA synthesis

Poly(ethylene glycol) monomethyl ether (**PEG$_{124}$-OH**) (1.48 g, 0.3 mmol), 4-cyano-4-[(dodecylsulfanylthiocarbonyl)sulfanyl]pentanoic acid (0.35 g, 0.87 mmol) and 4-(dimethylamino)pyridine (0.03 g, 0.24 mmol) were dissolved in dry dichloromethane (14 mL) under Ar atmosphere. After the solution was cooled to 0°C, *N,N'*-dicyclohexylcabodiimide (0.27 g, 1.3 mmol) was added. The solution was stirred at 0°C for 1 h, and then at room temperature for 24 h. The white precipitate was filtered off and the solvent was removed under vacuum. The crude product was precipitated twice into cold diethyl ether. The solid was centrifuged and dried. Poly(ethylene glycol) methyl ether 4-cyano-4-[(dodecylsulfanylthiocarbonyl)sulfanyl] pentanoate (**PEG$_{124}$-CTA**) was obtained as a yellow powder. Yield: 90%. FT-IR (KBr disk, cm^{-1}): 2885, 1970, 1761, 1467, 1360, 1342, 1280, 1242, 1150, 1106, 1060, 963, 947, 842. ^{1}H NMR (400 MHz, CDCl$_3$) δ (ppm): 4.25 (t, J = 4.8 Hz, 2H), 3.63 (s, 514H), 3.37 (s, 3H), 3.31 (t, J = 7.4 Hz, 2H), 2.66 (m, 2H), 2.57-2.31 (2H), 1.87 (s, 3H), 1.68 (qu, J = 4.7 Hz, 2H) 1.43-1.19 (20H), 0.87(t, J = 6.8 HZ, 3H). GPC (DMF): M$_n$ = 22605 g mol^{-1}; Đ = 1.07.

PEG$_{124}$-CTA (0.52 g, 0.10 mmol), monomer m**DAP** (0.36 g, 0.95 mmol), and AIBN (2.35 mg, 0.014 mmol) were added to a crimp vial and dissolved in dioxane (2.2 mL). The resulting solution was purged for 20 min with Ar and then placed into a preheated oil bath at 75°C. After 6 h, the reaction mixture was cooled down with an ice bath and exposed to air. The crude product was precipitated twice into cold diethyl ether. The solid was centrifuged and dried under vacuum overnight. **PEG$_{124}$-*b*-PDAP$_9$-CTA** was obtained as a slight yellow powder. Yield: 83%. Conversion: 93%. FT-IR (KBr disk, cm^{-1}): 3318, 2885, 1965, 1734, 1695, 1585, 1517, 1448, 1359, 1343, 1282, 1243, 1150, 1114, 1061, 964, 947, 842, 803. ^{1}H NMR (400 MHz, CDCl$_3$) δ (ppm): 8.97-8.23 (19H), 7.96-7.50 (29H), 4.42-4.05 (37H), 3.83-3.43 (528H), 3.37 (3H), 2.89-2.59 (37H), 2.44-2.27 (19H), 1.34-0.78 (65H). GPC (DMF): M$_n$ = 32910 g mol^{-1}; Đ = 1.18.

Seeded aqueous dispersion RAFT polymerization

The following representative protocol was used for the synthesis of **25-1**. **PEG$_{124}$-*b*-PDAP$_9$-CTA** (0.075 g, 8.0 µmol), HPMA (0.12 g, 0.83 mmol), VA-044 (0.8 mg, 2.5 µmol) were added into a 10 mL crimp vial and dissolved in distilled water (0.78 mL). Then, DMF (26 µL, 0.3 µmol) was added as internal standard for conversion calculation by ^{1}H NMR. In the case of one-pot PISA and supramolecular cross-linking, **T$_4$** was previously dissolved in this DMF adjusting its concentration to have stoichiometric 1:1 thymine-DAP ratio in the final dispersion; since **T$_4$** is able to interact with four DAP moieties, and considering that each polymer chain has an average of 9 DAP units, the calculated **T$_4$: PEG$_{124}$-*b*-PDAP$_9$-CTA** molar ratio was approx. 2.2:1. The mixture was degassed by bubbling Ar for 15 min. After this time, the vial was placed into a preheated oil bath at 50°C. After 5h, the vial was opened to air and allowed to cool down to room temperature. Conversion: >99%. ^{1}H NMR (400 MHz, MeOD) δ (ppm): 7.80-7.60 (29H), 4.40-4.09 (37H), 4.07-3.75 (281H), 3.68-3.51 (650H), 3.36 (s, 3H), 2.83-2.69 (39H), 2.48-2.37 (19H), 2.09-1.82 (160H), 1.37-0.82 (827H).

Nile Red encapsulation and release

100 µL of NR solution in DCM (0.035 mg mL^{-1}) were added to two flasks and then the solvent was evaporated. Afterwards, 11 mL of **10-1·T$_4$** diluted dispersion (1.04 mg mL^{-1}) was added into one of those flask and 10.32 mL of a **10-1** diluted dispersion (1.02 mg mL^{-1}) was added to the other one. In this way, the same polymer concentration, without taking into account **T$_4$**, (0.957 mg mL^{-1}) was achieved. The resulting dispersions were stirred 24 h at room temperature to reach equilibrium before fluorescence was measured (t = 0). After that, 0.5 mL of each solution were placed into a dialysis cup (Slide-A-Lyzer MINI Dialysis Device, 3.5K MWCO, 0.5 mL; ThermoFisher

Scientific) and dialyzed against Milli-Q® water (14 mL) at room temperature. At a given time, the sample was removed from the dialysis cup, fluorescence was measured and then it was given back to the dialysis cup. The emission spectra of NR were recorded from 565 to 800 nm while exciting at 550 nm.

Conclusions

Highly concentrated aqueous self-assemblies dispersions containing a non-water soluble nucleobase analogue (DAP) have been successfully prepared for the first time employing PISA methodology. To enable aqueous polymerization, an amphiphilic diblock copolymer composed by a PEG and a PDAP blocks was first synthesized by RAFT polymerization. This copolymer was easily dispersed in water and successfully used as macro-CTA for the aqueous seeded RAFT polymerization of HPMA.

By changing the length of the PHPMA block (series x = 1, 2 and 3) and the solids concentration (from 10 to 25 g / 100 mL), a phase diagram of these new **PEG$_{124}$-*b*-PDAP$_9$-*b*-PHPMA$_n$** formulations has been constructed. TEM and DLS studies indicated that the aqueous seeded RAFT polymerization of HPMA has led to aqueous self-assemblies dispersion with diverse morphologies (spherical micelles, worms and vesicles), which depended on the length of PHPMA block and solid concentration. The resulting self-assemblies dispersions are almost stable at least for 11 months, except in the case of worms' morphology, in which a transition to spherical micelles was progressively observed.

Incorporation of nucleobase analogue DAP units allows the supramolecular functionalization with thymine complementary derivatives by triple H-bonding. This possibility has been initially evaluated by incorporating a cross-linking agent with four terminal thymine groups (**T$_4$**) during aqueous seeded RAFT polymerization of HPMA. It was found that T$_4$ influenced the polymerization and the self-assembly morphologies. In addition, NR was successfully encapsulated as a hydrophobic molecular fluorescent probe by diffusion in both non-cross-linked and supramolecular cross-linked self-assemblies. For the later, a larger amount of NR could be encapsulated as well as a slower release was also observed. These preliminary results suggest a higher stability of the supramolecular cross-linked self-assemblies, evidencing the potential use of the system as nanocarriers.

Author Contributions

The manuscript was written through contributions of all authors.

Conflicts of interest

There are no conflicts to declare.

Acknowledgements

References

1 Y. Mai and A. Eisenberg, *Chem. Soc. Rev.*, 2012, **41**, 5969–5985.
2 H. Cabral, K. Miyata, K. Osada and K. Kataoka, *Chem. Rev.*, 2018, **118**, 6844–6892.
3 R. Fenyves, M. Schmutz, I. J. Horner, F. V. Bright and J. Rzayev, *J. Am. Chem. Soc.*, 2014, **136**, 7762–7770.
4 J. Dupont, G. Liu, K. I. Niihara, R. Kimoto and H. Jinnai, *Angew. Chemie - Int. Ed.*, 2009, **48**, 6144–6147.
5 A. Choucair, C. Lavigueur and A. Eisenberg, *Langmuir*, 2004, **20**, 3894–3900.
6 S. Li, J. He, M. Zhang, H. Wang and P. Ni, *Polym. Chem.*, 2016, **7**, 1773–1781.
7 M. Abad, G. Mendoza, L. Usón, M. Arruebo, M. Piñol, V. Sebastián and L. Oriol, *Macromol. Biosci.*, 2022, **22**, 2100528.
8 X. Wang and Z. An, *Macromol. Rapid Commun.*, 2019, **40**, 1–14.
9 S. L. Canning, G. N. Smith and S. P. Armes, *Macromolecules*, 2016, **49**, 1985–2001.
10 S. Y. Khor, J. F. Quinn, M. R. Whittaker, N. P. Truong and T. P. Davis, *Macromol. Rapid Commun.*, 2019, **40**, 1–22.
11 F. D'Agosto, J. Rieger and M. Lansalot, *Angew. Chemie Int. Ed.*, 2020, **59**, 8368–8392.
12 F. L. Hatton, M. J. Derry and S. P. Armes, *Polym. Chem.*, 2020, **11**, 6343–6355.
13 N. J. Warren, O. O. Mykhaylyk, D. Mahmood, A. J. Ryan and S. P. Armes, *J. Am. Chem. Soc.*, 2014, **136**, 1023–1033.
14 Y. Kang, A. Pitto-Barry, H. Willcock, W. D. Quan, N. Kirby, A. M. Sanchez and R. K. O'Reilly, *Polym. Chem.*, 2015, **6**, 106–117.
15 A. Blanazs, J. Madsen, G. Battaglia, A. J. Ryan and S. P. Armes, *J. Am. Chem. Soc.*, 2011, **133**, 16581–16587.
16 Y. Kang, A. Pitto-Barry, A. Maitland and R. K. O'Reilly, *Polym. Chem.*, 2015, **6**, 4984–4992.
17 L. D. Blackman, K. E. B. Doncom, M. I. Gibson and R. K. O'Reilly, *Polym. Chem.*, 2017, **8**, 2860–2871.
18 J. Rieger, *Macromol. Rapid Commun.*, 2015, **36**, 1458–1471.
19 S. Chen, P. Shi and W. Zhang, *Chinese J. Polym. Sci.*, 2017, **35**, 455–479.
20 C. J. Mable, K. L. Thompson, M. J. Derry, O. O. Mykhaylyk, B. P. Binks and S. P. Armes, *Macromolecules*, 2016, **49**, 7897–7907.
21 X. Shen, F. Huo, H. Kang, S. Zhang, J. Li and W. Zhang, *Polym. Chem.*, 2015, **6**, 3407–3414.
22 F. Huo, C. Gao, M. Dan, X. Xiao, Y. Su and W. Zhang, *Polym. Chem.*, 2014, **5**, 2736–2746.
23 P. Chambon, A. Blanazs, G. Battaglia and S. P. Armes, *Macromolecules*, 2012, **45**, 5081–5090.
24 M. Chen, J. W. Li, W. J. Zhang, C. Y. Hong and C. Y. Pan, *Macromolecules*, 2019, **52**, 1140–1149.
25 X. Dai, L. Yu, Y. Zhang, L. Zhang and J. Tan, *Macromolecules*, 2019, **52**, 7468–7476.
26 S. Sugihara, S. P. Armes, A. Blanazs and A. L. Lewis, *Soft Matter*, 2011, **7**, 10787–10793.
27 K. L. Thompson, C. J. Mable, A. Cockram, N. J. Warren, V. J. Cunningham, E. R. Jones, R. Verber and S. P. Armes, *Soft Matter*, 2014, **10**, 8615–8626.
28 Q. Zhang, R. Wang, Y. Chen, L. Zhang and J. Tan, *Langmuir*, 2022, **38**, 2699–2710.
29 J. R. Lovett, L. P. D. Ratcliffe, N. J. Warren, S. P. Armes, M. J. Smallridge, R. B. Cracknell and B. R. Saunders, *Macromolecules*, 2016, **49**, 2928–2941.
30 S. Varlas, J. C. Foster, P. G. Georgiou, R. Keogh, J. T. Husband, D. S. Williams and R. K. O'Reilly, *Nanoscale*, 2019, **11**, 12643–12654.
31 L. P. D. Ratcliffe, K. J. Bentley, R. Wehr, N. J. Warren, B. R. Saunders and S. P. Armes, *Polym. Chem.*, 2017, **8**, 5962–5971.
32 W. Zhou, Q. Qu, W. Yu and Z. An, *ACS Macro Lett.*, 2014, **3**, 1220–1224.
33 S. Xu, J. Yeow and C. Boyer, *ACS Macro Lett.*, 2018, **7**, 1376–1382.
34 M. Nardi, T. Scherer, L. Yang, C. Kübel, C. Barner-Kowollik and E. Blasco, *Polym. Chem.*, 2021, **12**, 1627–1634.
35 Q. Zhao, Q. Liu, C. Li, L. Cao, L. Ma, X. Wang and Y. Cai, *Chem. Commun.*, 2020, **56**, 4954–4957.

36 H. Yao, Y. Ning, C. P. Jesson, J. He, R. Deng, W. Tian and S. P. Armes, *ACS Macro Lett.*, 2017, **6**, 1379–1385.

37 X. Chen, L. Liu, M. Huo, M. Zeng, L. Peng, A. Feng, X. Wang and J. Yuan, *Angew. Chemie - Int. Ed.*, 2017, **56**, 16541–16545.

38 H. Khan, S. Chen, H. Zhou, S. Wang and W. Zhang, *Macromolecules*, 2017, **50**, 2794–2802.

39 E. Raphael, M. J. Derry, M. Hippler and S. P. Armes, *Chem. Sci.*, 2021, **12**, 12082–12091.

40 G. Mellot, J. M. Guigner, L. Bouteiller, F. Stoffelbach and J. Rieger, *Angew. Chemie Int. Ed.*, 2019, **58**, 3173–3177.

41 P. Gao, H. Cao, Y. Ding, M. Cai, Z. Cui, X. Lu and Y. Cai, *ACS Macro Lett.*, 2016, **5**, 1327–1331.

42 T. N. Tran, S. Piogé, L. Fontaine and S. Pascual, *Macromol. Rapid Commun.*, 2020, **41**, 1–5.

43 L. Romero-Azogil, N. J. W. Penfold and S. P. Armes, *Polym. Chem.*, 2020, **11**, 5040–5050.

44 J. Tan, D. Liu, Y. Bai, C. Huang, X. Li, J. He, Q. Xu, X. Zhang and L. Zhang, *Polym. Chem.*, 2017, **8**, 1315–1327.

45 N. Zaquen, J. Yeow, T. Junkers, C. Boyer and P. B. Zetterlund, *Macromolecules*, 2018, **51**, 5165–5172.

46 J. Tan, H. Sun, M. Yu, B. S. Sumerlin and L. Zhang, *ACS Macro Lett.*, 2015, **4**, 1249–1253.

47 J. Tan, Q. Xu, Y. Zhang, C. Huang, X. Li, J. He and L. Zhang, *Macromolecules*, 2018, **51**, 7396–7406.

48 N. J. W. Penfold, J. R. Whatley and S. P. Armes, *Macromolecules*, 2019, **52**, 1653–1662.

49 A. Concellón, R. Clavería-Gimeno, A. Velázquez-Campoy, O. Abian, M. Piñol and L. Oriol, *RSC Adv.*, 2016, **6**, 24066–24075.

50 A. Concellón, E. Blasco, A. Martínez-Felipe, J. C. Martínez, I. Šics, T. A. Ezquerra, A. Nogales, M. Piñol and L. Oriol, *Macromolecules*, 2016, **49**, 7825–7836.

51 M. Abad, A. Martínez-Bueno, G. Mendoza, M. Arruebo, L. Oriol, V. Sebastián and M. Piñol, *Polymers*, 2021, **13**, 684.

52 J. Milton Harris and R. B. Chess, *Nat. Rev. Drug Discov.*, 2003, **2**, 214–221.

53 T. Janoschka, A. Teichler, A. Krieg, M. D. Hager and U. S. Schubert, *J. Polym. Sci. Part A Polym. Chem.*, 2012, **50**, 1394–1407.

54 G. Moad, E. Rizzardo and S. H. Thang, in *Polymer Science: A Comprehensive Reference*, Elsevier, 2012, vol. 3, pp. 181–226.

55 A. Concellón, E. Blasco, M. Piñol, L. Oriol, I. Díez, C. Berges, C. Sánchez-Somolinos and R. Alcalá, *J. Polym. Sci. Part A Polym. Chem.*, 2014, **52**, 3173–3184.

56 T. J. Neal, N. J. W. Penfold and S. P. Armes, *Angew. Chemie Int. Ed.*, 2022, **61**, e202207376.

57 A. Blanazs, R. Verber, O. O. Mykhaylyk, A. J. Ryan, J. Z. Heath, C. W. I. Douglas and S. P. Armes, *J. Am. Chem. Soc.*, 2012, **134**, 9741–9748.